Theoretical Study on the Reaction Mechanism and Regioselectivity of Silastannation of Acetylenes with a Palladium Catalyst

Masahiko Hada, Yoko Tanaka, Mitsuru Ito, Masahiro Murakami, Hideki Amii, Yoshihiko Ito,* and Hiroshi Nakatsuji*,†

Contribution from the Department of Synthetic Chemistry and Biological Chemistry, Faculty of Engineering, Kyoto University, Kyoto, 606 Japan

Received April 11, 1994®

Abstract: A theoretical study on the reaction mechanism of the silastannation of various alkynes with a palladium catalyst is presented. We investigate the different regioselectivities in the reactions of SiH_3SnH_3 with monosubstituted acetylenes (CN, H, CH_3, and OCH_3) catalyzed by $Pd(PH_3)_2$. The overall reaction scheme is first examined, and then the factors for regioselectivities are analyzed. The rate-determining step is the insertion of acetylene into the Pd–Sn or Pd–Si bond of the complex. Three factors are pointed out as governing the reactivity and regioselectivity. The first is the electronic factor which determines the relative stabilities of the transition states (TS) involving differently oriented acetylenes and those of the regioisomeric intermediates obtained after the TS. The overall reactivity is determined by the electron back-donation from Pd (homo) to acetylene (lumo), while the stable orientation of the substituted acetylene is determined by the electron donation from the homo of acetylene to the lumo (localized on Sn or Si) of the Pd complex. The second is the steric hindrance of the ligands. The steric repulsion of PPh_3 of a $Pd(PPh_3)_4$ catalyst is large enough to give a different isomer from the one predicted by the electronic factor. The third is the occurrence of the thermodynamic control when the products after the TS are unstable and therefore the reverse reactions can easily occur. The regioselectivities reported experimentally and predicted theoretically here are reasonably explained by these three factors. The electron density distributions show electron donation and back-donation, supporting the electronic mechanism proposed in this paper. An agostic interaction, between palladium and hydrogen, is found in the intermediate after the insertion step.

1. Introduction

Organosilicon and tin compounds are important agents in organic syntheses, and their chemistry is well documented.[1] The bis-silylation,[2] bis-stannylation,[3] and silastannation[4] reactions which give regioselective and stereoselective products have been investigated for 10 years. New synthetic methods of interest have also been developed using these silicon- and tin-containing compounds.[5]

In this paper, our interest is mainly focused on the regioselectivity of the silastannation reactions. Chenard *et al.* have reported that terminal acetylenes react with silylstannanes to give highly regio- and stereoselective 1-silyl-2-stannylalkenes by using tetrakis(triphenylphosphine)palladium as a catalyst.[4c] The products are always cis adducts; tin adds to the internal position as follows:

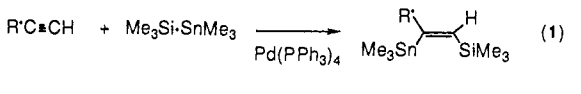

(1)

where R′ is a phenyl, alkyl, or silyl group. Mitchell *et al.* have also independently reported equivalent results.[4d] Recently, Ito *et al.* reported that alkoxyacetylenes react with various silylstannanes to give regio- and stereoselective 1-silyl-2-stannylalkenes using the palladium acetate–*tert*-alkyl isocyanide catalyst:[6]

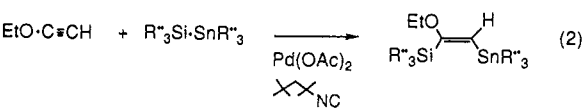

(2)

The regioselectivity in this reaction is opposite to that in eq 1. However, the reaction of alkylacetylenes with the use of the palladium–isocyanide catalyst gives the products given by the eq 1. These different regioselectivities are difficult to explain by a single reaction mechanism. Further, Mitchell *et al.* reported that some internal acetylenes having both phenyl and ester groups react with silylstannanes,[4d] but the regioselectivity was poor. Bis-

† Also belongs to the Institute for Fundamental Chemistry, Nishihiraki-cho, Sakyo-ku, Kyoto, 606 Japan.

® Abstract published in *Advance ACS Abstracts*, August 15, 1994.

(1) (a) *The Chemistry of Organic Silicon Compounds*; Patai, S., Rappoport, Z., Eds.; Wiley-Interscience: Chichester, U.K., 1989. (b) *Chemistry of Tin*; Harrison, P. G., Ed.; Blackie: Glasgow, 1989.

(2) (a) Okinoshima, H.; Yamamoto, K.; Kumada, M. *J. Organomet. Chem.* **1975**, *86*, C27. (b) Sakurai, H.; Kamiyama, Y.; Nakadaira, Y. *J. Am. Chem. Soc.* **1975**, *97*, 931. (c) Tamao, K.; Hayashi, M.; Kumada, M. *J. Organomet. Chem.* **1976**, *114*, C19. (d) Watanabe, H.; Kobayashi, M.; Higuchi, K.; Nagai, Y. *J. Organomet. Chem.* **1980**, *186*, 51. (e) Watanabe, H.; Kobayashi, M.; Saito, M.; Nagai, Y. *J. Organomet. Chem.* **1981**, *216*, 149. (f) Watanabe, H.; Saito, M.; Sutou, N.; Kishimoto, K.; Inose, J.; Nagai, Y. *Ibid.* **1982**, *225*, 343. (g) Hayashi, T.; Kobayashi, T.; Kawamoto, A. M.; Yamashita, H.; Tanaka, M. *Organometallics* **1990**, *9*, 280.

(3) (a) Mitchell, T. N.; Amamria, A.; Killing, H.; Rutschow, D. *J. Organomet. Chem.* **1983**, *241*, C45. (b) Killing, H.; Mitchell, T. N. *Organometallics* **1984**, *3*, 1318. (c) Piers, E.; Skerlj, R. T. *J. Chem. Soc., Chem Commun.* **1986**, 626.

(4) (a) Mitchell, T. N.; Killing, H.; Dicke, R.; Wickenkamp, R. *J. Chem. Soc., Chem. Commun.* **1985**, 354. (b) Chenard, B. L.; Laganis, E. D.; Davidson, F.; RajanBabu, T. V. *J. Org. Chem.* **1985**, *50*, 3666. (c) Chenard, B. L.; Van Zyl, C. M. *J. Org. Chem.* **1986**, *51*, 3561. (d) Mitchell, T. N.; Wickenkamp, R.; Amamria, A.; Dicke, R.; Schneider, U. *J. Org. Chem.* **1987**, *52*, 4868.

(5) (a) Ito, Y.; Bando, T.; Matsuura, T.; Ishikawa, M. *J. Chem. Soc., Chem. Commun.* **1986**, 980. (b) Chanard, B. L.; Van Zyl, C. M.; Sanderson, D. R. *Tetrahedron Lett.* **1986**, *27*, 2801. (c) Mitchell, T. N.; Schneider, U. *J. Organomet. Chem.* **1991**, *407*, 319. (d) Mori, M.; Kaneta, N.; Shibasaki, M. *J. Org. Chem.* **1991**, *56*, 3486. (e) Mori, M.; Watanabe, N.; Kaneta, N.; Shibasaki, M. *Chem. Lett.* **1991**, 1615. (f) Tsuji, Y.; Obora, Y. *J. Am. Chem. Soc.* **1991**, *113*, 9368. (g) Tsuji, Y.; Kakehi, T. *J. Chem. Soc., Chem. Commun.* **1992**, 1000. (h) Ito, Y.; Suginome, M.; Murakami, M. *J. Org. Chem.* **1991**, *56*, 1948. (i) Ikenaga, K.; Hiramatsu, K.; Nasaka, N.; Matsumoto, S. *J. Org. Chem.* **1993**, *58*, 5045. (j) Obora, Y.; Tsuji, Y.; Asayama, M.; Kawamura, T. *Organometallics* **1993**, *12*, 4697.

(6) Murakami, M.; Amii, H.; Takizawa, N.; Ito, Y. *Organometallics* **1993**, *12*, 4223.

0002-7863/94/1516-8754$04.50/0

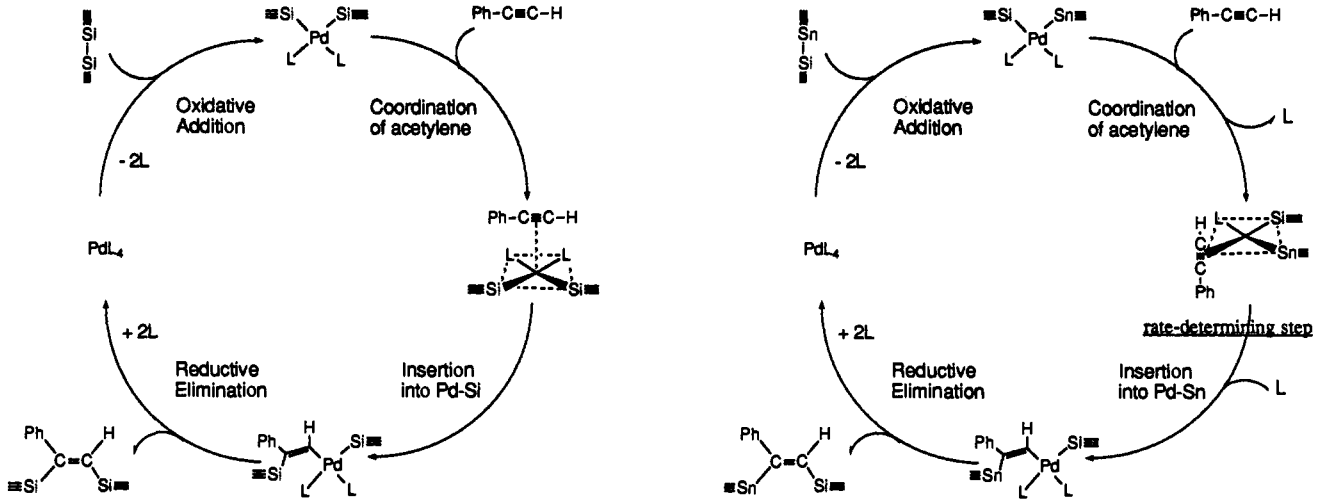

A B

Figure 1. Reaction scheme (A) suggested by Nagai *et al.*[2d] for bis-silylation and (B) adopted in this paper for silastannation.

silylation of acetylenes with unsymmetrically substituted disilanes can give a regioselective product.[2d]

The regio- and stereoselectivities of the above-described reactions include much information of importance to clarify the reaction mechanism; however, these have not yet been fully understood. A possible reaction scheme for the bis-silylation of acetylenes has been suggested by Nagai *et al.*[2d] and is shown in Figure 1A. In this scheme, a disilane oxidatively adds to a palladium complex, then an acetylene coordinates to it, the acetylene inserts into the Pd—Si bond, and finally the SiH_3 on Pd and the C=C part are coupled and reductively eliminated from the Pd complex. A similar reaction scheme for the bis-silylation of ethylenes with a platinum complex has been suggested by Hayashi *et al.*[2g] The reaction scheme which is adopted in this paper is also shown in Figure 1B. There are some differences to be pointed out in these two schemes.

Many theoretical investigations have been reported for the reactions involving the various transition metal complexes, for example, for the oxidative additions of H–H,[7-10] C–H,[11] C–C,[11] and Si–H[12] and for the insertions of CO[13] and olefins.[14,15] Recently electron correlation effects have been examined even for the transition metal complexes of considerable size.[16,17]

In this paper, we investigate the silastannation in which nonsubstituted silylstannane reacts with various monosubstituted acetylenes. In the next section, we show the reaction model and the method of calculations. In section 3, we study the energy diagram for the overall reaction scheme in order to examine whether the reaction scheme proposed for the bis-silylation is acceptable for the silastannation reaction. In sections 4–8, we discuss the reactivity and regioselectivity and point out three governing factors. The first factor, which we discuss in sections 4–6, is the electronic interactions between the highest occupied molecular orbitals (homo's) and the lowest unoccupied molecular orbitals (lumo's) of the acetylene and the palladium complex. The energy diagrams in the rate-determining step are given in section 4. We show the orbital correlation diagrams and discuss the electronic mechanism in section 5. The electron density maps are analyzed in section 6. The second factor is the steric repulsion between the substituent of acetylene and the ligand of the Pd complex, which we discuss in section 7. The third factor is the thermodynamic vs kinetic control in the reaction step involving the transition states, which we discuss in section 8.

2. Reaction Model and Computational Methods

The model reactions which we adopt in this paper are shown below. Two regioisomers specified by the positions of Sn and Si are given as

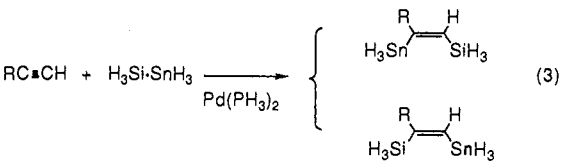

(3)

where R = CN, H, CH_3, and OCH_3. As a silylstannane we use SiH_3SnH_3. The substituents of H_3Si–SnH_3 are not considered in this paper because the reactivities of Si and Sn are expected to be different enough to give the regioselectivity. As a model catalyst, we use $Pd(PH_3)_2$, which has smaller steric hindrances than $Pd(PPh_3)_2$. We believe that the electronic effects on the reactivities and the regioselectivities of various substituted acetylenes are reproduced by this model system. The steric effects are examined separately in section 5. We also investigate the hydrosilylation in which acetylene inserts into a Si–H bond of SiH_4 to compare the contour maps of the electron densities.

We carried out ab-initio Hartree–Fock calculations to determine the structures and energies of all the intermediates and some transition states (TS) which appear along the reaction scheme. The basis sets used in our calculations are double-ζ quality on every atom, augmented with d polarization functions on the central atoms. The details are described in Appendix 1. Electron correlation effects are also discussed in the typical case (R = CH_3), and these results are given in Appendix 1.

3. Overall Reaction Scheme

As shown in Figure 1, the bis-silylation reaction involves the following steps: (a) oxidative addition, (b) coordination of

(7) Kitaura, K.; Obara, S.; Morokuma, K. *J. Am. Chem. Soc.* **1981**, *103*, 2891.
(8) Low, J. J.; Goddard, W. A., III *J. Am. Chem. Soc.* **1984**, *106*, 6928, 8321.
(9) Hay, P. J. *Chem. Phys. Lett.* **1984**, *103*, 466.
(10) Brandemark, U. K.; Blomberg, M. R. A. *J. Phys. Chem.* **1984**, *88*, 4617.
(11) Balazs, A. C.; Johnson, K. H.; Whitesides, G. M. *Inorg. Chem.* **1982**, *21*, 2162.
(12) Sakaki, S.; Ieki, M. *J. Am. Chem. Soc.* **1991**, *113*, 5063.
(13) Sakaki, S.; Kitaura, K.; Morokuma, K.; Obara, K. *J. Am. Chem. Soc.* **1983**, *105*, 2280.
(14) Daniel, C.; Koga, N.; Han, J.; Fu, X. Y.; Morokuma, K. *J. Am. Chem. Soc.* **1988**, *110*, 3773.
(15) Koga, N.; Jin, S. Q.; Morokuma, K. *J. Am. Chem. Soc.* **1988**, *110*, 3417.
(16) Sakaki, S.; Koga, N.; Morokuma, K. *Inorg. Chem.* **1990**, *29*, 3110.
(17) Sakaki, S.; Ieki, M. *Inorg. Chem.* **1991**, *30*, 4218.

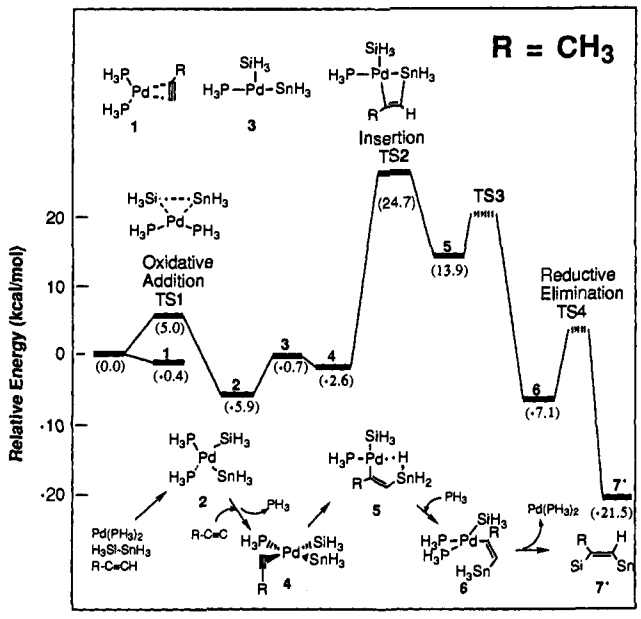

Figure 2. Reaction scheme and energy diagram for silastannation of methylacetylene. Values in parentheses are the energies relative to those of the initial compounds: $Pd(PH_3)_2$ + H_3Si–SnH_3 + methylacetylene. For calculating the relative energies of **1**–**5**, a free H_3Si–SnH_3 and a free PH_3 are considered. Adduct **3** is not a transition state, but its energy level gives the upper limit for exchanging ligands. Energy levels shown by broken lines (**TS3** and **TS4**) are calculated by the estimated geometries.

acetylene, (c) insertion of acetylene into Pd–Si, and (d) reductive elimination. We examine whether this reaction scheme is acceptable for the silastannation of acetylenes. (Triphenylphosphine)palladium(0) has the structure of $Pd(PPh_3)_4$ in a crystal, but $Pd(PPh_3)_2$ also exists in solution as an equilibrium species.[18] $Pd(PPh_3)_2$ is assumed to work as the catalyst in Figure 1. Therefore, palladium has two PH_3 ligands at the first stage in our calculations. The coordination number of palladium is also examined.

Figure 2 shows the energy diagram along the overall silastannation reaction pathway. Geometrical parameters are optimized under the C_s symmetry. To investigate the overall reaction scheme, we considered the reaction of methylacetylene with H_3SiSnH_3 which gives 1-silyl-2-stannyl-1-propene. The reaction scheme adopted in this paper is shown inside Figure 2. The compound number and the transition state number **TS***n* (n = 1–4) are also defined in the figure. The same notations are commonly used for the reactions of acetylene and methyl-, methoxy-, and cyanoacetylenes. This diagram shows that this reaction is 21.5 kcal/mol exothermic. According to the Nagai's scheme, the first stage is the oxidative addition of H_3Si–SnH_3 to Pd.[2d] Adduct **2** is 5.9 kcal/mol more stable than the initial separated molecules. Then PH_3 is replaced with methylacetylene to give adduct **4**. The energy level of the transition state for exchanging ligands should be lower than that of **3**. Next, acetylene inserts into the Pd–Sn bond. This transition state is at the highest energy level in this diagram, so this insertion would be the rate-determining step of the reaction. The geometry of this transition state should be closely related to the regioselectivity of the reaction. After the insertion, PH_3 adds to Pd again and the ethylene and Si reductively eliminate from the palladium complex. The reaction from **5** to **7** is greatly exothermic. As a whole, the reaction scheme shown inside Figure 2 is possible judging from the overall energy shape.

We note that the palladium complex has only one PH_3 ligand from **4** to **5**. It is essentially square planar in **4** and **TS2**. Even after the insertion, in **5**, the Pd keeps four coordination by interacting strongly with H of the SnH_3 group. This agostic interaction has been reported theoretically in the other reactions.[19]

Some other reaction pathways exist as possible candidates. In particular, the five-coordinate palladium complexes and the coordination of acetylene prior to the oxidative addition of H_3Si–SnH_3 should be considered. The present calculation shows that the five-coordinate complex $Pd(SiH_3)(SnH_3)(PH_3)_3$ is unstable: one PH_3 group spontaneously eliminates from the complex. $Pd(SiH_3)(SnH_3)(PH_3)_2$(acetylene) is also unstable. Therefore, four coordination would be a maximum, though PH_3 is a weaker ligand than PPh_3. Methylacetylene coordinates to $Pd(PH_3)_2$, giving adduct **1**, though it is unstable in comparison with adduct **2**. Adduct **1** is not an efficient reagent for the oxidative addition of H_3Si–SnH_3 because after the oxidative addition it becomes the pentacoordinate complex, which is unstable as described above.

Ozawa *et al.*[20] suggested that the reductive elimination might occur from the three-coordinate complexes, and Tatsumi *et al.*[21] also reported theoretically that ethane reductively eliminates from the T-shaped $Pd(PH_3)(CH_3)_2$ through the Y-shaped complex. However, the present calculations show that the four-coordinate complex is much more stable than the three-coordinate one as shown in Figure 2.

In the following sections, we study the rate-determining step involving compounds **4**, **5**, and **TS2** for various substituted acetylenes and study the origin of the reactivity and regioselectivity.

4. Energy Profiles around the Insertion Step

From the energetics of the overall reaction, it is clear that the reactivity and the regioselectivity are determined in **TS2**, which is the insertion step of the acetylenes into Pd–Sn or Pd–Si. In this section, the energy profiles around the insertion step are shown for the acetylenes substituted with R = CN, H, CH_3, or OCH_3. The result of this section is the basis for discussing the electronic mechanism in the next section.

Figure 3 shows possible reaction schemes in which acetylene with substituent R inserts into either of the Pd–Si or Pd–Sn bond. The reaction scheme is initially divided into two pathways (one for **4a** and one for **4b**). Acetylene and Sn occupy the cis positions in **4a**, and so acetylene inserts into the Pd–Sn bond, while acetylene and Si occupy the cis positions in **4b**, and therefore acetylene inserts into the Pd–Si bond. Each of the intermediates, **4a** and **4b**, gives two transition states, **TS2x**-α and **TS2x**-β (**x** = **a**, **b**), where α and β indicate that Si or Sn adds to the internal carbon (α-carbon) or to the terminal carbon (β-carbon), respectively. As a result, there are four possible geometries for the transition states, **TS2a**-α, **TS2a**-β, **TS2b**-α, and **TS2b**-β, which lead to the four corresponding regioisomeric intermediates **5x**-y (**x** = **a**, **b**; y = α, β). **TS2a**-α and **Ts2b**-β give the same product **7**, while **TS2a**-β and **TS2b**-α give **7′**, at the final stage.

The energy profiles involving **4x**, **5x**-y, and **TS2x**-y (**x** = **a**, **b**; y = α, β) for R = CN, CH_3, H, and OCH_3 are shown in Figure 4. Fully optimized geometries and their geometrical parameters are shown in Figures 14, 15, and 16 in Appendix 3. The structures of **TS2x**-y (**x** = **a**, **b**; y = α, β) are optimized under C_s symmetry. The structures of TS2 in C_s and C_1 symmetries are compared in Appendix 2, suggesting that the C_s symmetry is a good approximation for TS2.

In Figure 4, the energy levels of intermediates **4a**,**b** are taken as a standard. In fact, the energy levels of **4a**,**b** were essentially

(18) Maitlis, P. M.; Espinet, P.; Russell, M. J. H. Complexes of Palladium(0). In *Comprehensive Organometallic Chemistry*; Wilkinson, G., Stone, F. G. A., Abel, E. W., Eds.; Pergamon Press: Oxford, U.K., 1982; Vol. 6, Chapter 38.9.

(19) Koga, N.; Obara, S.; Kitaura, S.; Morokuma, K. *J. Am. Chem. Soc.* **1985**, *107*, 7109.

(20) Ozawa, F.; Ito, T.; Nakamura, Y.; Yamamoto, A. *Bull. Chem. Soc. Jpn.* **1981**, *54*, 1868.

(21) Tatsumi, K.; Hoffmann, R.; Yamamoto, A.; Stille, J. K. *Bull. Chem. Soc. Jpn.* **1981**, *54*, 1857.

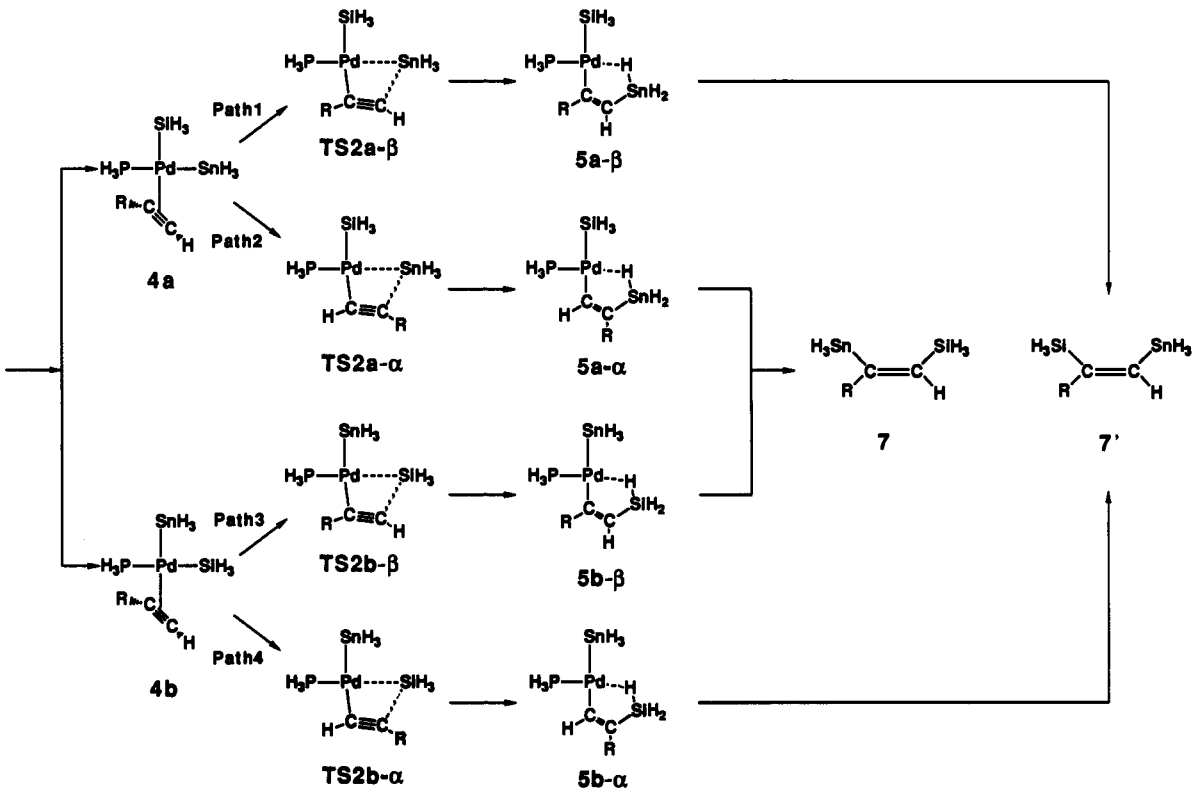

Figure 3. Possible reaction schemes for the insertion step. Acetylenes substituted by R insert into the Pd–Sn bond (top) or the Pd–Si bond (bottom). The α and β indicate at which carbon the addition of Si or Sn occurs.

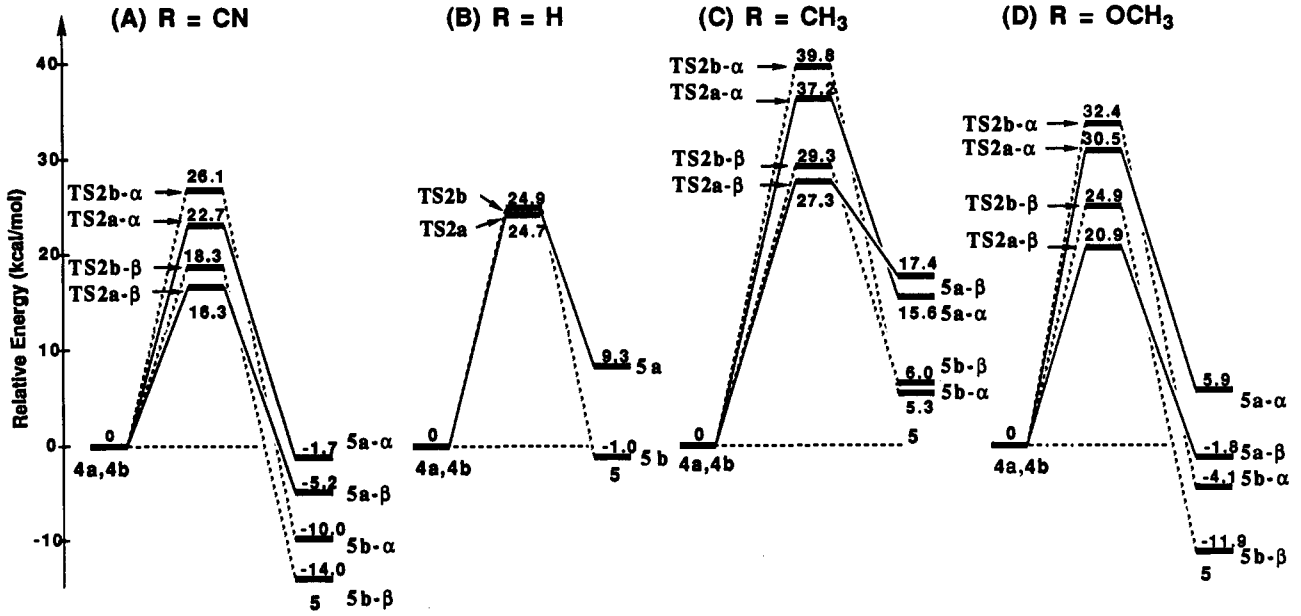

Figure 4. Energy profiles for the insertion step. The energy levels of the transition states **TS2x**-y and the adducts **4x** and **5x**-y (x = **a**, **b**; y = α, β) are shown. Values are the relative energies in kcal/mol. The substituents R are (A) CN, (B) H, (C) CH_3, and (D) OCH_3.

the same. We can divide the energy levels of **TS2** into two groups, stable and unstable. The stable group contains **TS2x**-β (x = **a**, **b**) and the unstable one contains **TS2x**-α (x = **a**, **b**), which indicates that the position of the substituent in acetylene controls the major stability of TS2. The addition of Si or Sn to the terminal carbon of acetylene occurs more easily than that to the internal carbon. Further, there are two sublevels in both groups which are controlled by the factor that the addition of Sn is preferable to the addition of Si. As a result, **TS2a**-β is the most stable of the four **TS2**'s for all the compounds studied here (R = CN, H, CH_3, and OCH_3).

The relative stabilities in adduct **5** are not the same as in **TS2**. Here the major factor is the difference between the Si–C and Sn–C bond energies, the former being larger than the latter. Therefore **5b**-y (y = α, β) are always more stable than **5a**-y (y = α, β). The relative orientation of the substituted acetylene is a minor factor for the stability of the intermediates.

A. Cyanoacetylene. Figure 4A shows the energy diagram for cyanoacetylene (R = CN). The activation energy for **TS2a**-β is 16.3 kcal/mol, which shows that cyanoacetylene is most reactive of all the species studied in this paper. All four pathways from **4** to **5** are exothermic. The compounds **5b**-y are more stable than **5a**-y (y = α, β) as described above.

B. Acetylene. Figure 4B shows the results for nonsubstituted acetylene, and so no difference exists between α and β. Two reaction pathways going through **TS2a** and **TS2b** have essentially the same activation energy, and therefore, the insertions into the Pd–Si and Pd–Sn bonds are not significantly different for

Table 1. Activation Energy for the Insertion Step and the Energy Split between **TS2a**-α and **TS2a**-β (kcal/mol)[a]

substituent	lowest activation energy	energy split (**TS2a**-α/**TS2a**-β)[b]	energy split (**TS2a**-β/**TS2b**-β)[c]
H	24.1		
CH_3	27.3	9.9	2.0
OCH_3	20.9	9.6	4.0
CN	16.3	6.4	2.0

[a] The definition of **TS2x**-y (**x** = **a**, **b**; y = a, b) is shown in Figure 3. [b] The energy difference between **TS2a**-α and **TS2a**-β. [c] The energy difference between **TS2a**-β and **TS2b**-β.

nonsubstituted acetylene, though those for compounds **5a**,**b** are very different in energy.

C. Methylacetylene. Figure 4C is for methylacetylene (R = CH_3). The methyl group is an electron-donating substituent, in contrast to the CN group which is an electron-withdrawing substituent. The energy levels of **TS2** are in the same order as those of Figure 4A. The activation energy in **TS2a**-β is calculated to be 27.3 kcal/mol, and therefore, methylacetylene would be less reactive than acetylene and cyanoacetylene. In the case of methylacetylene, it should be pointed out that compounds **5** are less stable than compounds **4**. The reverse reaction is facilitated if compounds **5** are populated. This point is important and will be discussed in detail in section 8.

D. Methoxyacetylene. Figure 4D is for methoxyacetylene (R = OCH_3). The energy levels of **TS2** are, again, in the same order as those for cyanoacetylene and methylacetylene, shown in Figure 4A,C. The smallest activation energy is 20.9 kcal/mol, and therefore, methoxyacetylene is expected to be less reactive than cyanoacetylene and to be more reactive than methylacetylene.

Adducts **5b**-y (y = α, β) are more stable than **5a**-y (y = α, β) in every acetylene of Figure 4. The position of the substituents does not make a large difference in the energy; therefore, the order of **5x**-α and **5x**-β (x = a,b) is not always the same in Figure 4A,C,D.

The activation energies and the energy differences between **TSa**-α and **TSa**-β and between **TSa**-β and **TSb**-β are summarized in Table 1. The activation energies increase in the order CN < OCH_3 < H < CH_3. We expect that the reactivity follows the same ordering. The energy differences between **TS2a**-α and **TS2a**-β increase in the order CN < OCH_3 < CH_3. This indicates the electronic effects of the differently oriented acetylenes. The energy differences between **TS2a**-y and **TS2b**-y (y = α, β) indicate that the insertion into Pd–Sn is preferable to that into Pd–Si. These differences are smaller than those between **TS2a**-α and **TS2a**-β as shown in Table 1. The electronic mechanisms of these results will be discussed below.

5. Electronic Mechanism

In this section we discuss the electronic origin for the variations in the energy levels shown in Figure 4. These energy levels mainly reflect the electronic effects because PH_3 has a small steric effect. Nagai *et al.*[2d] suggested that the charges $\delta+$ and $\delta-$ on the internal and terminal carbons of acetylene play an important role for the regioselectivity in the bis-silylation reaction with unsymmetrically substituted disilanes. However, this simple charge control cannot explain the regioselectivity, as shown in eqs 1 and 2. The relative stability of the products cannot explain it either. This reaction seems to be governed by the frontier control, as will be shown below by examining the electronic mechanism.

A. Orbital Correlation between Acetylene and Palladium. First, we examine the behaviors of the π and π^* orbitals of acetylene upon substitution. The π and π^* orbitals are the highest occupied molecular orbital (homo) and the lowest unoccupied molecular orbital (lumo), respectively. The energy levels of the π and π^* orbitals for R = CN, H, CH_3, and OCH_3 and their shapes are shown in Figure 5. The acetylenes are bent by about 50° to mimic the electronic structure in the transition state. We will

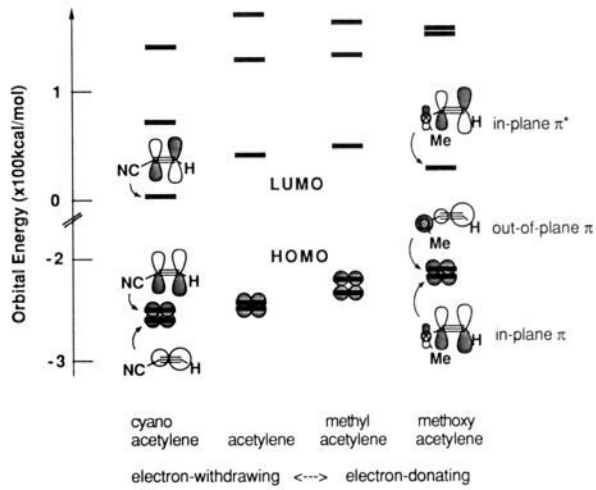

Figure 5. Orbital energy levels of the nonsubstituted and substituted acetylenes. Each acetylene is bent by about 50° to mimic the electronic state in the transition state.

briefly explain the well-known substituent effect of the electron-donating group (CH_3 or OCH_3) and the electron-withdrawing group (CN) relative to hydrogen.[22] The π orbital is destabilized in methyl- and methoxyacetylene, while it is stabilized in cyanoacetylene. The π^* orbital of cyanoacetylene is lower in energy than those of methyl- and methoxyacetylene. This shows that cyanoacetylene is a stronger electrophile than methyl- and methoxyacetylene and that methyl- and methoxyacetylene are stronger nucleophiles than cyanoacetylene. The bent structures of the acetylenes emphasize these effects on the energy. The substituents polarize the homo (π) and lumo (π^*) as shown in Figure 5. In general, the substituents having two π electrons enlarge the coefficient of the terminal π orbital of the homo, irrespective of the substituents. This polarization can be more easily understood from the shape of the nonbonding π orbital of allyl anion, which has a node at the central carbon, rather than the substituent effect on the acetylene π-MO. The in-plane π^* orbitals are polarized toward the terminal carbon, though the extent is small. The out-of-plane π^* orbitals are always much higher in energy than the in-plane ones and therefore can be ignored.

Figure 6 shows the orbital correlation diagram between methoxyacetylene and the palladium complex. The geometries used in this diagram are those in **TS2a**-β, with the distance between acetylene and Pd elongated to 3 Å. At the **TS2** geometry, the electronic interaction is too large to see a simple orbital correlation. The homo and the next homo of acetylene interact with the lumo and the next lumo of the palladium complex, respectively. The resultant orbitals, 28 and 29, are stabilized in comparison with the initial π orbitals, 14 and 15, of acetylene. Through this orbital interaction, acetylene donates an electron to the palladium complex, particularly, to the Sn atom. The homo of the palladium complex also interacts with the π^* (lumo) of acetylene. The resultant orbital, 31, is not stabilized, suggesting that this interaction is still small at this stage. The orbital correlation diagram for methylacetylene is similar to that for methoxyacetylene. Figure 7 shows the orbital correlation diagram between cyanoacetylene and the palladium complex. The geometry is chosen in the same manner as explained for Figure 6. As the π^* orbital (lumo) of the cyanoacetylene is much lower in energy than those of methyl- and methoxyacetylene, the electron back-donating interaction from Pd to acetylene becomes large: the resultant orbital, 29, in Figure 7 is greatly stabilized in comparison with the corresponding orbital, 31, in Figure 6.

B. Two Governing Factors for Reactivity and Regioselectivity. Since **TS2a**-β is the most stable in Figure 4 and the terminal π

(22) *Frontier Orbitals and Organic Chemical Reactions*, Fleming, I., Ed.; Wiley-Interscience, William Clowes & Sons, Ltd.: London, 1976.

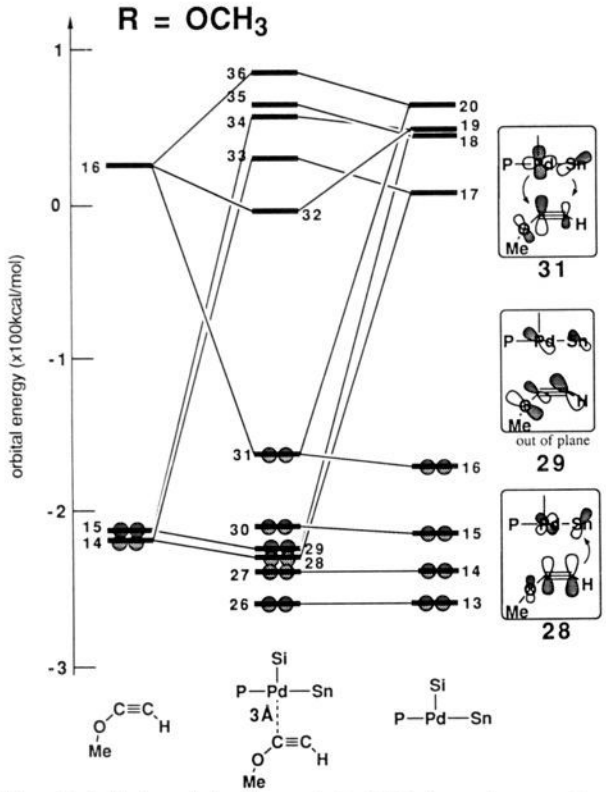

Figure 6. Orbital correlation diagram before **TS2** when methoxyacetylene interacts with the palladium complex. They are separated by 3 Å, keeping the geometries in the transition state. The acetylene donates an electron to the palladium complex through the 28th orbital, and the palladium complex back-donates an electron to the acetylene through the 31st orbital.

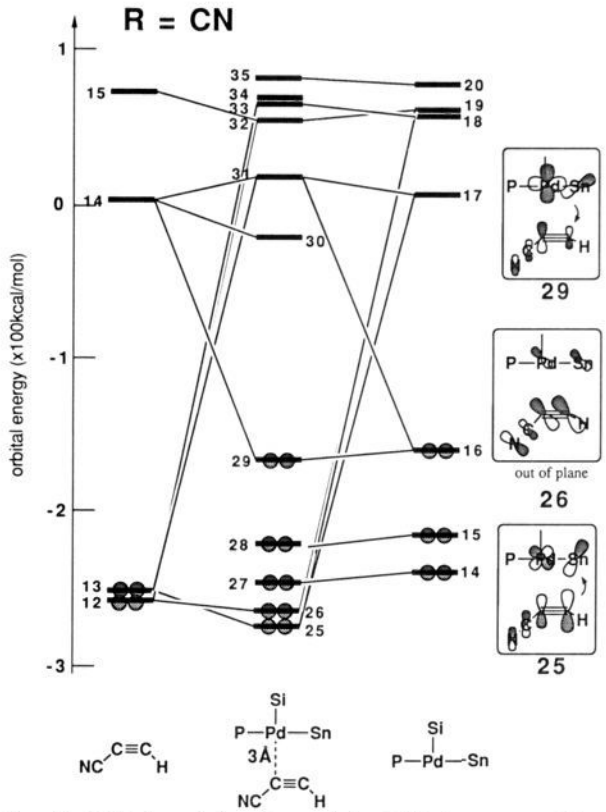

Figure 7. Orbital correlation diagram before **TS2** when cyanoacetylene interacts with the palladium complex. They are separated by 3 Å, keeping the geometries in the transition state. The acetylene donates an electron to the palladium complex through the 25th orbital, and the palladium complex back-donates an electron to the acetylene through the 29th orbital.

electron of the substituted acetylene is enriched, the orientation of acetylene in **TS2** seems to be governed by the π orbital (homo) of acetylene donating an electron to Sn. In cyanoacetylene, the energy difference between **TS2a**-α and **TS2a**-β is relatively small in comparison with methyl- and methoxyacetylene. This is because the π orbital of cyanoacetylene is stable and inactive, as shown in Figure 5, so that the electronic control for the orientation of cyanoacetylene is weak. There is no clear evidence showing that the electron back-donation from the Pd complex to acetylene is related to the orientation of acetylene. The polarization of the π^* orbital is not large and seems to be opposite to the orientation of acetylene, as the electron back-donation occurs from Pd and Sn to acetylene. Nevertheless, the electron back-donation is important to stabilize **TS2** regardless of the orientation of acetylenes. The activation energies in Table 1 are in the same order as the π^* orbital (lumo) energy levels in Figure 5.

Judging from the results described above, we conclude that there are two governing factors in the electronic mechanism of this reaction. One is concerned with the lumo of acetylene: the electron back-donation from the homo of the Pd complex, which is mainly the Pd d orbital bonding with the Sn p orbital, to the lumo π^* of acetylene. This interaction is illustrated below on the right-hand side. This governs the reactivity of the substituted acetylenes: the stability of **TS2** shown in Figure 4 parallels the stability of the lumo level of the substituted acetylene. This is energetically the largest interaction. The other factor is related to the homo of acetylene: the electron donation from the homo of acetylene to the lumo of the Pd complex, which is the vacant p orbital localized on Sn. This is illustrated below on the left-hand side. It governs the orientation of acetylene; namely, the terminal carbon having the larger homo (π) coefficient interacts with Sn.

The presence of two governing factors may seem strange since in most reactions one governing homo–lumo interaction determines both reactivity and selectivity. The back-donating interaction is energetically the most important but is insensitive to the orientation. The donating interaction is sensitive to the orientation though energetically less important. The reason is explained by the following orbital interaction picture:

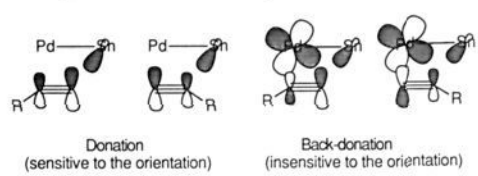

In the donating interaction, the π orbital (homo) of acetylene interacts with the 3p orbital of Sn, so the orientation of acetylene becomes important when it is strongly polarized. However, in the back-donating interaction, the 4d orbital of Pd is spacially large and interacts with both inner and outer p orbitals of the lumo of acetylene, as shown in the above diagram, and so this interaction is insensitive to the orientation of acetylene or the polarization of its π^* orbital.

C. Route in the Insertion Step: Into Pd–Sn or into Pd–Si? The insertion of acetylenes into Pd–Sn is easier than that into Pd–Si, though this selectivity is small energetically, as shown in Table 1 and Figure 4. It is due to the difference in the electrophilicity between Si and Sn and/or in the stability between highly coordinated Si and Sn. The electronic mechanism described above may be applied to explain the observation[2d] that the Si substituted by methoxy groups, expected to behave like Sn, adds to the internal carbon in the bis-silylation. The structures of the pentacoordinate Si and Sn in **TS2** are not clear trigonal bipyramids, as shown in Appendix 3.

6. Electron Density Distribution

In this section, to analyze the nature of the interaction between acetylene and the palladium complex, we show the contour maps

Figure 8. Contour maps of electron density difference $\Delta\rho$ for methylacetylene at the transition state (right) and before the transition state (left). In the early interaction state (left), the separation between methylacetylene and the palladium complex is 1 Å longer than that in the transition state (right).

Figure 9. Contour maps of electron density difference $\Delta\rho$ for methoxyacetylene at the transition state (right) and before the transition state (left). In the early interaction state (left), the separation between methoxyacetylene and the palladium complex is 1 Å longer than that in the transition state (right).

of the electron density difference $\Delta\rho$, which is defined by

$$\Delta\rho = \rho(\text{total}) - \rho(\text{acetylene}) - \rho(\text{palladium complex}) \quad (4)$$

where ρ(total) is the total electron density of the system and ρ(moiety) is the electron density of the moiety calculated as an isolated molecule. Therefore, $\Delta\rho$ shows the reorganization of the electron distribution when the acetylene interacts with the Pd complex. The geometry of each part is taken from the geometry in **TS2a**-β, which is the most stable. The contour maps for methyl-, methoxy-, and cyanoacetylenes are shown in Figures 8, 9, and 10, respectively. In the left map, the distance of acetylene and the palladium complex is elongated by 1 Å from the transition state, keeping the other geometrical parameters fixed, so we can observe the early interaction before the transition state. The right map is drawn at the transition state.

In Figures 8, 9, and 10, the situations around Pd and acetylene are similar. In the left maps, the electron density around the right carbon decreases while that of the left carbon bonded to Pd increases. This change in electron density clearly represents the electron donation and back-donation between the acetylene and the palladium complex, as explained above by the orbital correlation diagram. The acetylene donates an electron to Sn, and the Pd back-donates it to the acetylene. The decrease of electron density at the right carbon implies that the Sn atom works as an electrophile and that it interacts with the π electron of the acetylene. The behavior of ρ of the Pd complex looks more complicated. In the right maps, the electron density increases on both the carbons of acetylene. In these structures, the electron back-donation seems to be important. Evidence of Pd–C and Sn–C bonding is observed, and the electron density at the Pd–Sn bonding region decreases, suggesting that the Pd–Sn bond is broken in the following step. The C–C bonds of the acetylenes are also weakened in the right maps. The pentacoordinate character of Sn is not as prominent in these figures, as in the structures shown in Figures 14, 15, and 16 of Appendix 3.

For comparing the interactions on Pd–SnH_3 and Pd–H, we show in Figure 11 the contour maps of $\Delta\rho$ for the insertion of methoxyacetylene into the Pd–H bond. This transition state

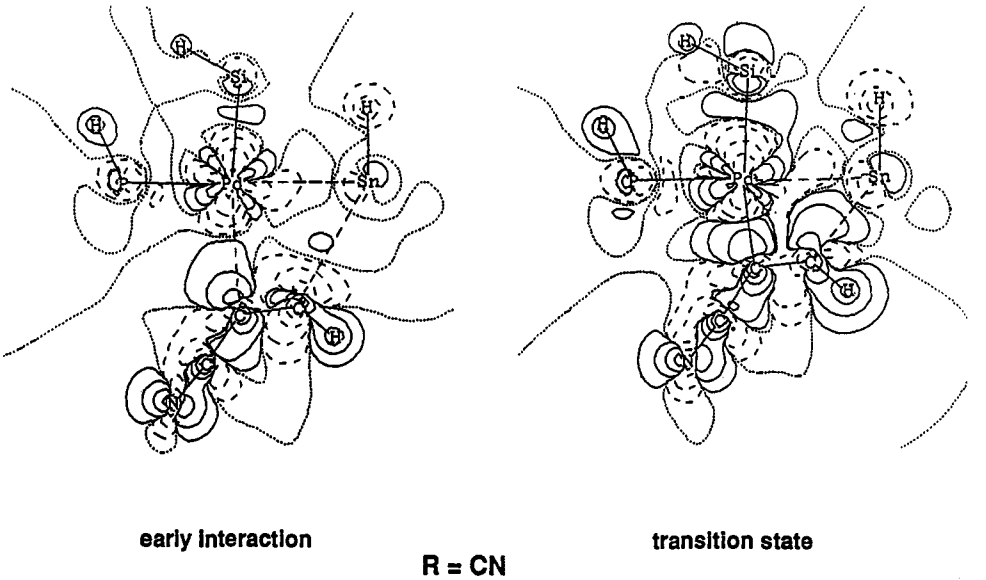

Figure 10. Contour maps of electron density difference $\Delta\rho$ for cyanoacetylene at the transition state (right) and before the transition state (left). In the early interaction state (left), the separation bewteen cyanoacetylene and the palladium complex is 1 Å longer than that in the transition state (right).

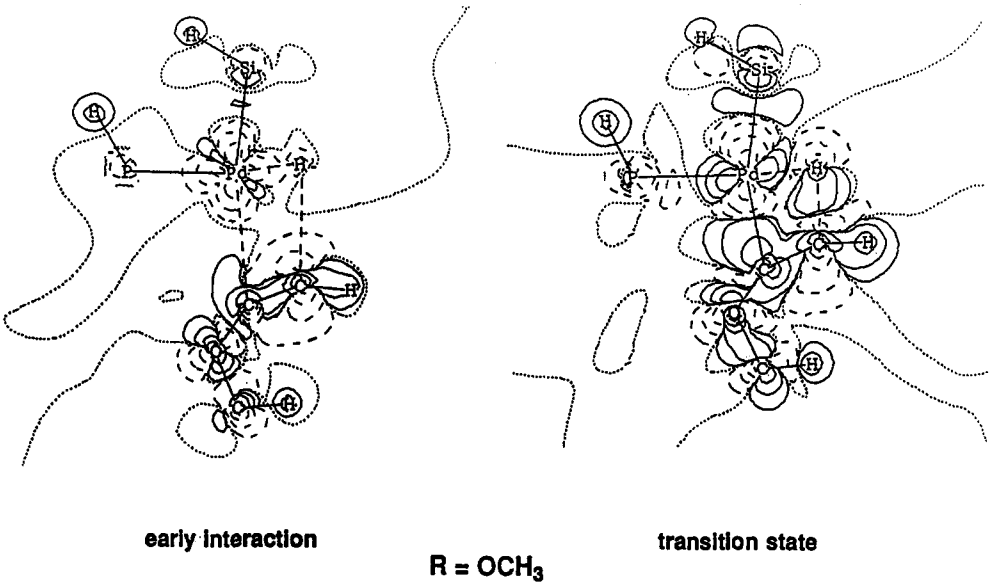

Figure 11. Contour maps of electron density difference $\Delta\rho$ for the insertion of methoxyacetylene into the Pd–H bond at the transition state (right) and before the transition state (left). In the early interaction state (left), the separation between methoxyacetylene and the palladium complex is 1 Å longer than that in the transition state (right).

appears in the hydrosilylation of acetylene. The structures of the corresponding **TS2** and **5** are shown in the Figure 12. In the left map, the electron distribution around acetylene is similar to that in Figure 9, though the electron transfer is smaller. In the right map, the electron density around H is clearly polarized toward the carbon of the acetylene. The hydrogen s orbital has no specific direction so that the electron density around H can be polarized easily to the preferable direction. In Figure 9, the electron distribution around the Sn–C bond is polarized to the Pd–Sn bond and/or the Pd–C bond. The activation energy is 20.9 kcal/mol in the insertion step into Pd–H, which is comparable with that into Pd–Sn.

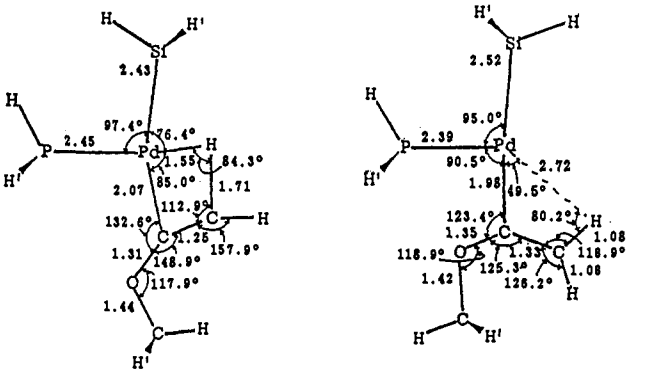

Figure 12. Structures of the transition state and the inserted product **5** in hydrosilylation (R = OCH_3). H′ indicates the two hydrogens above and below the plane.

7. Steric Effect

Judging from the results of the electronic interaction shown in section 4, the reaction always proceeds through **TS2a**-β and therefore tin always adds to the terminal carbon of the substituted acetylenes. This explains the experimental regioselectivity for eq 2 of the Introduction but not for eq 1. The steric effect seems to be important when $Pd(PPh_3)_4$ is used as a catalyst instead of $Pd(PH_3)$ as used here. In order to investigate this steric effect,

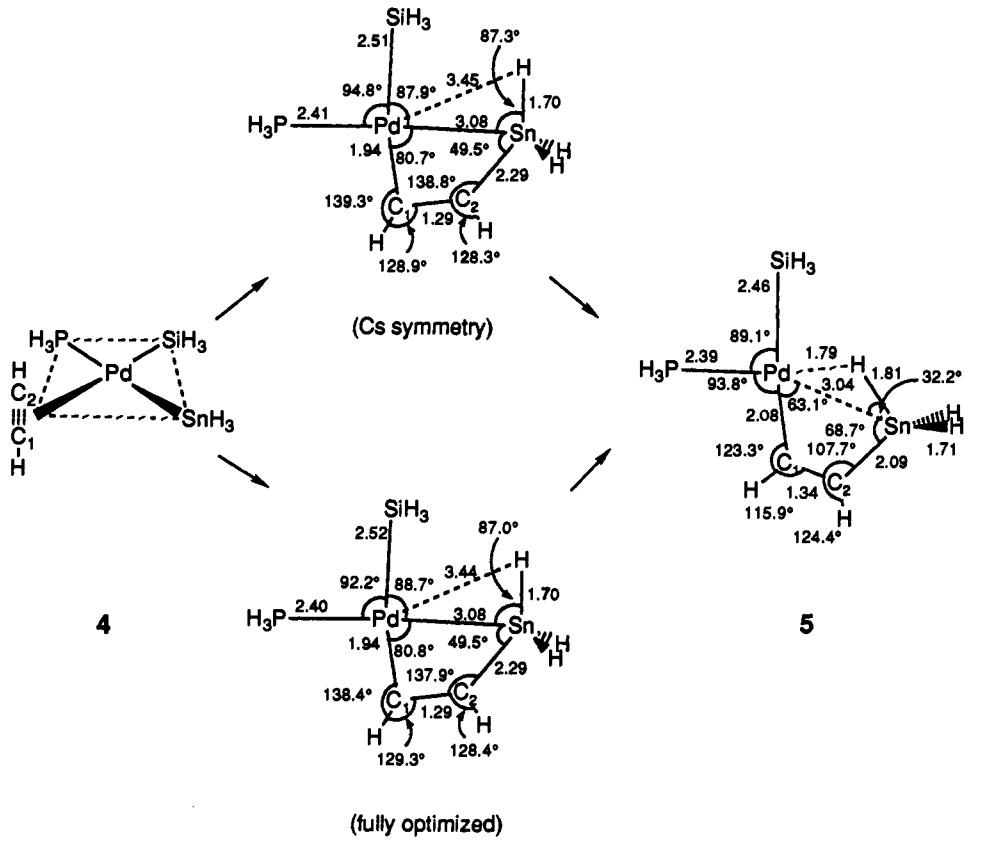

Figure 13. Schematic pictures and the optimized geometries of adducts **4** and **5** and the transition state **TS2** (R = H). It is assumed that acetylene inserts into the Pd–Sn bond in **TS2**. The geometry for **TS2** is optimized fully, keeping the C_s symmetry for comparison. The activation energies in this step are 24.1 kcal/mol (fully optimized) and 24.7 kcal/mol (C_s).

we replace PH_3 with PPh_3 in **TS2** of methylacetylene. The geometry is optimized by using the smaller basis set (BS-II, in Appendix 1), fixing the geometrical parameters of PPh_3, SiH_3, SnH_3, and CH_3. As a result, **TS2a**-α becomes more stable by 12.6 kcal/mol than **TS2a**-β, which is reverse to the previous

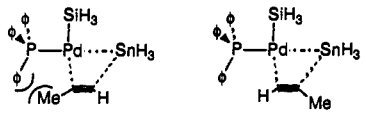

results for the PH_3 ligand shown in Figure 4. It shows that the steric effect of PPh_3 is large enough to give the opposite regioisomer regardless of the electronic control. So we conclude that Sn always adds to the internal carbon of acetylene when $Pd(PPh_3)_4$ is used as a catalyst.

This large steric hindrance of the PPh_3 group may be synthetically useful for always obtaining a special isomer. However, for obtaining a different isomer and for giving the chemistry of the silastannation greater variety, we suggest the use of less bulky ligands in the palladium complex. Then, we expect that the electronic control described above (and also the thermodynamic control described below) would work to give individual products.

In this sense, the palladium–isocyanide catalysts[5,6] are interesting. The steric effect involved in the reaction using this catalyst seems to be much smaller than that in the (triphenylphosphine)-palladium catalyst because the Pd–C–N–C part would seem to be linear in the complex. We discuss this point in the next section.

8. Thermodynamic Control vs Kinetic Control

From the shapes of the potential diagrams in Figure 4, we should consider that this reaction is controled thermodynamically in the case of methylacetylene because adducts **5** are less stable than **4**. Two typical cases follow, in which the kinetic control and the thermodynamic control are predominant, respectively:

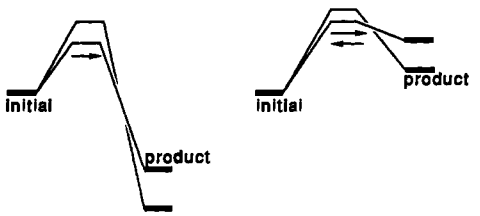

When the product is much more stable than the initial compound, the relative height in the activation energy determines the reaction pathway. On the other hand, when the product is less stable and the activation energy is small and when the equilibrium between the initial and final compounds exists, the selectivity should be determined by the relative stability of the products. **TS3** in Figure 2 plays a role in populating **5x**-y (**x** = **a**, **b**; y = α, β) after **TS2**. In Figure 4C, the initial adducts **4a,b** are more stable than the products **5**, while in Figure 4A,D, the products **5** are more stable than **4**. Therefore the thermodynamic control and the kinetic control would work for methyl- and methoxyacetylene, respectively. In this discussion, we consider only the lower two reaction pathways (**TS2a**-β and **TS2b**-β) and neglect the higher two ones. As a result, we expect that **5a**-β in Figure 4A,D and **5b**-β in Figure 4C are the main products when there are no steric effects. This result agrees with the experimental results for methyl- and methoxyacetylene with a Pd–isocyanide catalyst. For cyanoacetylene, no experiments have not yet been done but we expect the same regioselectivity as for methoxyacetylene. However, the energy difference between **TS2a**-α and **TS2a**-β is small, and therefore, the regioselectivity would not be very high.

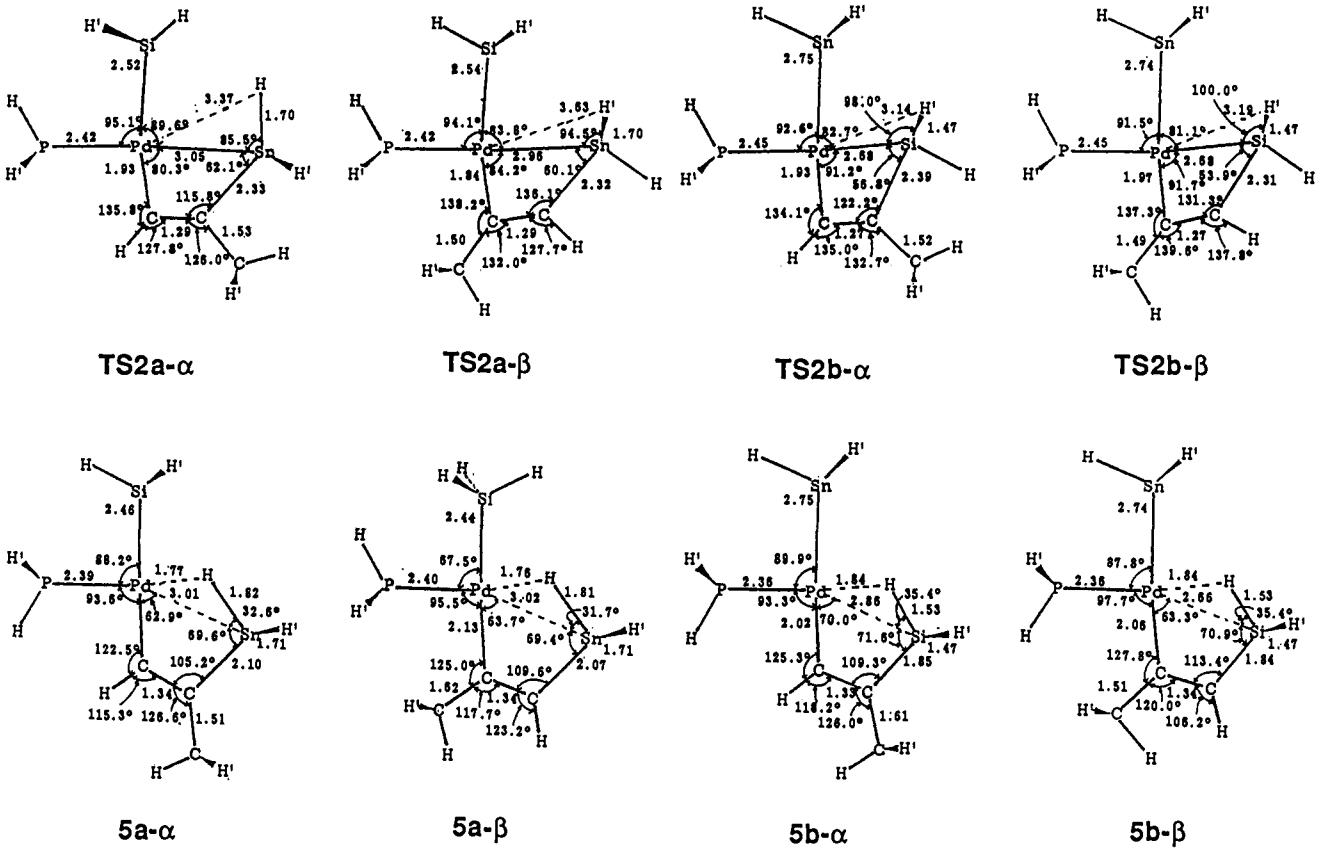

Figure 14. Optimized structures of the transition states and products **5** inserted in methylacetylene. **TS2x-y** and **5x-y** (**x** = **a**, **b**; y = α, β) are defined in Figure 3. H′ indicates the two hydrogens above and below the plane.

The Pd–isocyanide complex has much smaller steric hindrances than the $Pd(PPh_3)_2$ complex, so that this complex is believed to work as a catalyst without the steric hindrance. Actually, using the Pd–isocyanide catalyst, Sn adds to the terminal carbon of alkoxyacetylene, while it adds to the internal carbon of alkylacetylene.[6] If we are able to extend the present results to the Pd–isocyanide catalyst, these different regioselectivities may be explained by the kinetic (frontier) control and the thermodynamic control.

9. Concluding Remarks

We have studied the reaction mechanism for the silastannation of various alkynes with a palladium catalyst. We first examined the overall reaction scheme, and the results are summarized as follows.

(1) The reaction scheme presented in this paper is similar to, but different in some details from, the reaction scheme suggested by Nagai *et al.*[2d] for the bis-silylation reaction.

(2) $Pd(PH_3)_2$ works as a catalyst, SiH_3SnH_3 easily adds oxidatively to the catalyst, and acetylene adds to the catalyst causing one PH_3 ligand to leave.

(3) The rate-determining step in this reaction scheme is the insertion of acetylene into Pd–Sn or Pd–Si. The palladium complex around the insertion step is essentially four-coordinate square planer.

Three factors are important in determining the reactivity and the regioselectivity of this reaction. They are summarized as follows.

(a) Electronic Effect. (1) The orientation of acetylene is determined by the electron-donating interaction from the homo (π) of acetylene to the lumo of the palladium complex which is localized on Sn. Monosubstituted acetylene prefers to orient with the terminal carbon to Sn.

(2) The electron back-donating interaction from the homo of the Pd complex, which is mainly the d orbital of Pd, to the lumo (π^*) of acetylene is energetically important but is insensitive to the orientation of acetylene. This interaction controls the reactivity of the substituted acetylene but does not cause the regioselectivity.

(3) The insertion of acetylene into Pd–Sn is preferable to that into Pd–Si because of the larger electrophilicity of Sn.

(b) Steric Repulsion. The steric repulsion between the PPh_3 ligand of the $P(PPh_3)_4$ complex and CH_3 in $CH_3C{\equiv}CH$ is large enough to determine the orientation of this acetylene regardless of the electronic effect described above. Therefore, in the reaction using $Pd(PPh_3)_4$ as a catalyst, the steric effect controls the regioselectivity, so that Sn always adds to the internal carbon of the substituted acetylenes.

(c) Thermodynamic Control. (1) Thermodynamic control becomes important when the reaction intermediates after the rate-determining TS barrier are less stable than the initial compounds. Therefore, in the case of methylacetylene, the regioselectivity is determined by the relative stability of the intermediates after the TS.

(2) The regioselectivities of methylacetylene and methoxyacetylene using the Pd–isocyanide catalyst, which has small steric effect, are due to the thermodynamic control and kinetic control, respectively.

Acknowledgment. Part of the calculations have been carried out with the computers at the Data Processing Center of Kyoto University and at the Institute for Molecular Science. We thank the IMS computer center for the grant of computing time. Part of this study has been supported by a Grant-in-Aid for Scientific Research from the Japanese Ministry of Education, Science, and Culture and by CIBA-GEIGY Foundation (Japan) for the Promotion of Science.

Appendix 1: Basis Set and Electron Correlation Effect

Calculations in this paper were carried out by the ab-initio Hartree–Fock SCF method. Basis functions used in this calculation are summarized in Table 2. They are valence double-ζ

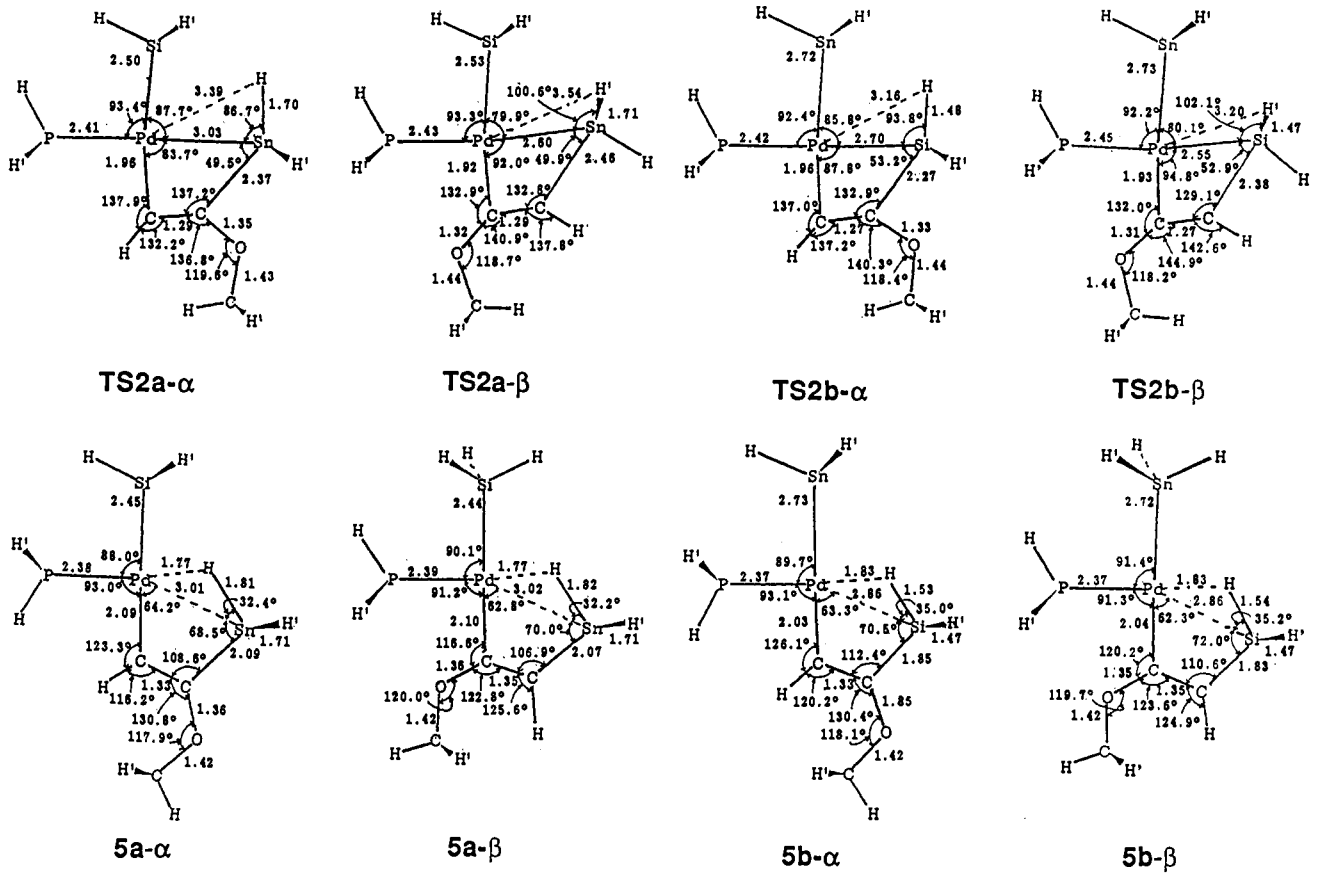

Figure 15. Optimized structures of the transition states and products **5** inserted in methoxyacetylene. **TS2x-y** and **5x-y** (x = **a**, **b**; y = α, β) are defined in Figure 3. H′ indicates the two hydrogens above and below the plane.

Table 2. Basis Functions (Basis Set I)

atom	basis set (s/p/d)	ECP[a]
Pd	(111/21/31)[a]	Kr core
Sn	(21/21)[a] + d(0.262)[b]	Ne core
Si	(21/21)[a] + d(0.183)[b]	Kr core
P	(21/21)[a]	Ne core
C (acetylene)	4-31G[c] + d(0.60)[b]	
C (methyl)	4-31G[c]	
O	4-31G[c]	
N	4-31G[c]	
H (H–C)	(31)[d]	
H (H–Pd)	(31/31)[d,e]	

[a] Reference 23. [b] Reference 24. [c] Reference 25. [d] Reference 26. [e] As polarization functions, the derivatives of 1s(H) are added on H (ref 27).

functions[23-26] augmented with the polarization d functions[24] on Si, Sn, and C atoms which play an important role in the reaction process. The derivatives of 1s(H) are added as polarization functions[27] on H for hydrosilylation. The core electrons of Pd, P, Si, and Sn are replaced with the effective core potentials (ECP) proposed by Hay and Wadt.[23] This basis set is called BS-I in this paper. Main parts of our calculations were performed by BS-I. For checking the electron correlation effects and the steric effects of the ligands, we used the smaller basis set in which all polarization d functions are removed from BS-I, and this basis function is called BS-II. The program used in this paper is Gaussian 92.[28]

Table 3. Some Important Geometrical Parameters and Relative Energies[a] of **4a** and **5a**-β (R = CH_3) by the RHF, MP2, and MP4 Theories

		BS-I[b]	BS-II[b]		
molecule	term	RHF	RHF	MP2	MP4/MP2[c]
4a	Pd–Sn	2.58	2.57	2.59	
	Pd–Si	2.33	2.35	2.40	
	Pd–P	2.67	2.66	2.53	
	Pd–C_1	2.79	2.68	2.35	
	PdC_1C_2	62.8	83.5	77.1	
	$PPdC_1C_2$	97.7	99.9	113.6	
5a-β	Pd–Sn	3.02	3.05	2.63	
	Pd–Si	2.44	2.45	2.69	
	Pd–P	2.40	2.39	2.49	
	Pd–H	1.76	1.79	1.75	
	Pd–C_1	2.13	2.13	2.11	
	PdC_1C_2	117.4	116.6	118.8	
	$PPdC_1C_2$	178.8	178.9	180.2	
relative energy[d]		17.4	16.4	13.8	12.6

[a] Bond lengths in Å, angles in deg, and energies in kcal/mol. [b] BS-I and BS-II mean large and small basis sets, respectively. See text for details. [c] Single-point MP4 calculation at the geometry optimized by MP2. [d] Relative to **4a**.

Table 3 shows some geometrical parameters and energetics of compound **5a**-β relative to **4a** (R = CH_3) calculated by the RHF and MP2 methods. BS-II is used for this check. The energies are also calculated by the MP4 method at the geometries optimized by the MP2 method, which is indicated as MP4/MP2. The optimized bond lengths are quite similar among the RHF(BS-I), RHF(BS-II), and MP2(BS-II) calculations, while the angles are somewhat different among these methods. The relative energies

(23) Hay, P. J.; Wadt, W. R. *J. Chem. Phys.* **1985**, *82*, 270.
(24) Huzinaga, S., Ed. Gaussian basis sets for molecular calculations. In *Physical Science Data 16*; Elsevier Science Publishers B.V.: Amsterdam, 1984.
(25) Ditchfield, R.; Hehre, W. J.; Pople, J. A. *J. Chem. Phys.* **1971**, *54*, 724.
(26) Dunning, T. H., Jr.; Hay, P. J. *Modern Theoretical Chemistry*; Schaefer, H. F., III, Ed.; Plenum: New York, 1977; Vol. 4, Chapter 1.
(27) (a) Nakatsuji, H.; Kanda, K.; Yonezawa, T. *Chem. Phys. Lett.* **1980**, *75*, 340. (b) Nakatsuji, H.; Kanda, K.; Yonezawa, T. *J. Chem. Phys.* **1982**, *77*, 3109.
(28) Frisch, M. J.; Gordon, M. H.; Trucks, G. W.; Foresman, J. B.; Schlegel, H. B.; Raghavachari, K.; Robb, M. A.; Binkley, J. S.; Gonzalez, C.; Defrees, D. J.; Fox, D. J.; Whiteside, R. A.; Seeger, R.; Melius, C. F.; Baker, J.; Martin, R. L.; Kahn, L. R.; Stewart, J. J. P.; Topiol, S.; Pople, J. *Gaussian 92*: Gaussian, Inc.: Pittsburgh, PA, 1992.

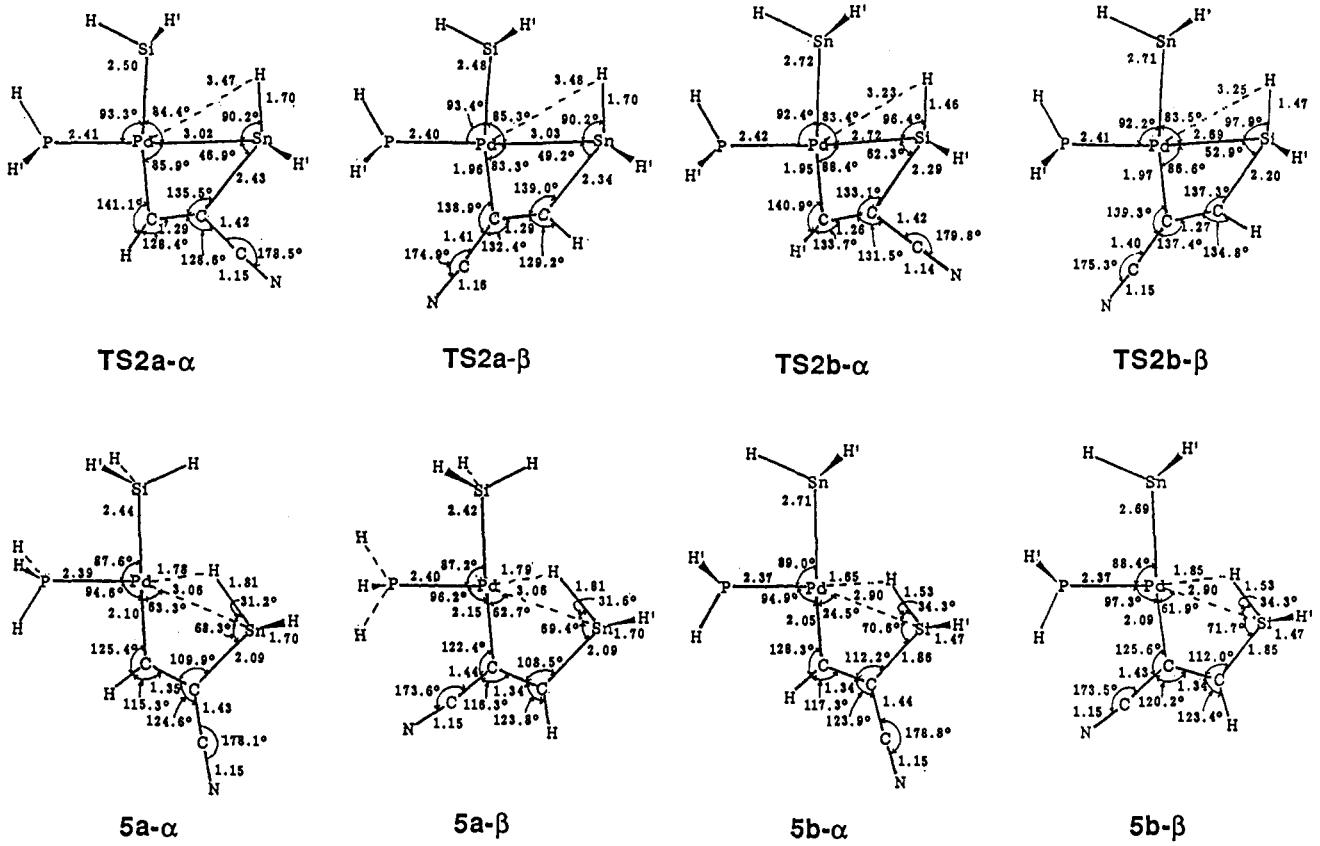

Figure 16. Optimized structures of the transition states and products 5 inserted in cyanoacetylene. **TS2x**-y and **5x**-y (x = **a**, **b**; y = α, β) are defined in Figure 3. H′ indicates the two hydrogens above and below the plane.

between **4a** and **5a**-β do not differ much. We therefore believe that the RHF calculations for **4x** and **5x**-y (x = **a**, **b**; y = α, β) are reliable.

The **TS2a**-β is calculated to be 10.7 kcal/mol more stable than **TS2a**-α by the MP4(BS-I)/RHF(BS-I), while 9.9 kcal/mol by RHF(BS-I). Therefore the relative stabilities for the differently oriented acetylene in **TS2** may be reproduced by the MP4 method. However, using the geometries optimized by the RHF method in the calculations including electron correlations is not necessarily adequate especially around the transition states. With our computational facilities, it is difficult to calculate optimized geometries of the transition states using correlated wave functions.

Appendix 2: Transition States in C_1 and C_s Symmetries

The transition state (**TS2**) between the adducts **4** and **5** is mainly investigated in this paper because the regioselectivity is determined in this step as described above. We restricted the geometries of the transition states (**TS2**) to have the C_s symmetry. We show here that the C_s geometry is located reasonably close to the C_1 geometry, which is the fully optimized one. This check was carried out for nonsubstituted acetylene. Figure 13 shows the pertinent geometries in which it is assumed that the acetylene inserts into the Pd–Sn bond in **TS2**. The dihedral angles θ between the Sn–Pd–C_1 and the Pd–C_1–C_2 planes and between the P–Pd–Si and Pd–Si–Sn planes are 1.1° and 180.6°, respectively, so all atoms except for some H atoms are essentially on the same plane. The reaction mode, given by the eigenvector corresponding to the negative eigenvalue of the Hessian matrix, is mainly the Pd–Sn vibration and Pd–C_1–C_2 bending. This motion occurs in plane. Fully optimized geometrical parameters are also shown in Figure 13. The activation energy is 24.1 kcal/mol. When the geometry of **TS2** is restricted to keep C_s symmetry, the activation energy is 24.7 kcal/mol. This deviation in energy is very small. The geometrical parameters of the C_s transition state are also shown in Figure 13, and they are essentially the same as those obtained for the C_1 symmetry. So, it is safe to restrict the geometry of **TS2** to be C_s.

Appendix 3: Optimized Structures

The optimized geometrical parameters of the complexes for R = CH_3, OCH_3, and CN are shown in Figures 14, 15, and 16. All **TS2**'s are essentially square planar. The agostic interaction is always observed in compounds **5**. After passing the transition states, the Pd–Sn or Pd–Si bond seems to be replaced by the Pd–H bond, keeping the square planar configuration. The Pd–Sn distances are 2.8–3.1 Å in **TS2** and 3.0 Å in **5**, while the Pd–Si distances are 2.5–2.7 Å in **TS2** and 2.8–2.9 Å in **5**. They do not change much from **TS2** to **5**, i.e. the Si and Sn atoms just move around the Pd atom after **TS2**. Both Si and Sn are pentacoordinate in **TS2**, though they are distorted trigonal bipyramids. They seem to be the tetrahedral structure in the bond alternating process. The stability in high coordination is significant for the allylation reaction reported previously;[29] it may not be so in this reaction. As there are two possible conformations for the SiH_3 and SnH_3 groups in **TS2** with C_s symmetry, we always adopted the most stable conformation.

(29) Hada, M.; Nakatsuji, H.; Ushio, J.; Izawa, M.; Yokono, H. *Organometallics* **1993**, *12*, 3398.